

SUPPLEMENTAL MATERIALS

S1: CORROSION MEASUREMENTS SETUP

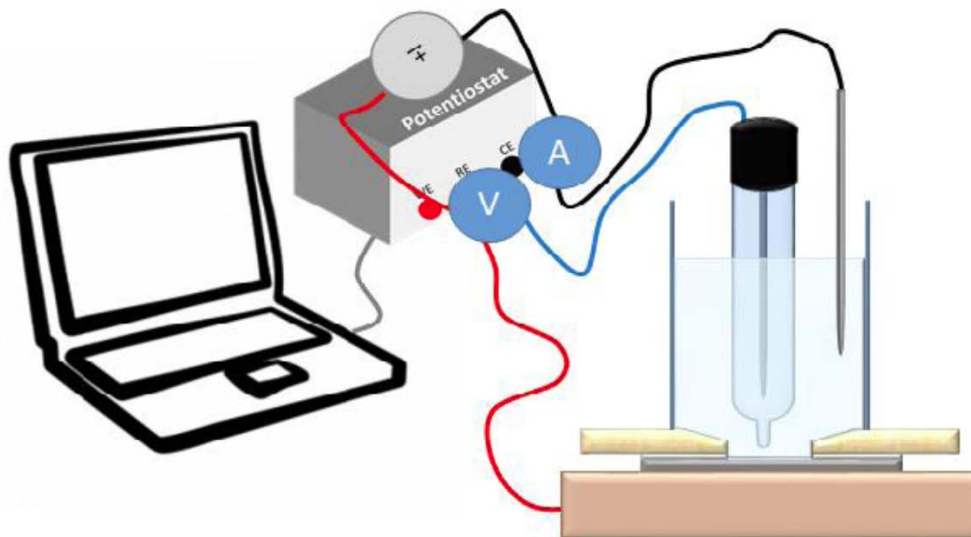


Figure S1: The corrosion measurement setup.

S2: SPECTROSCOPIC DATA

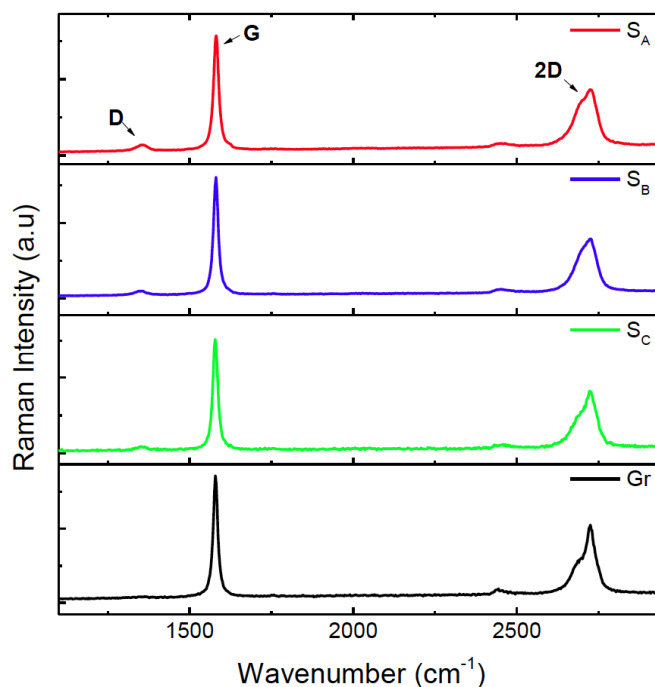
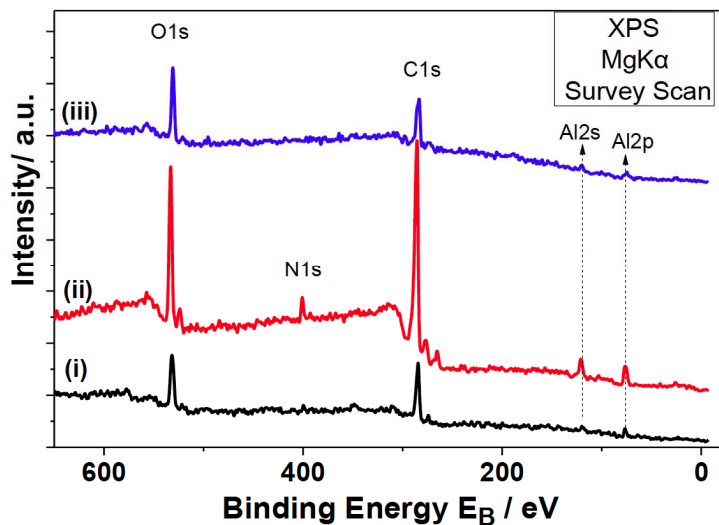


Figure S2: Typical Raman spectra for the commercial Al foils samples (S_A , S_B , S_C) coated with GRMs as well as graphite.

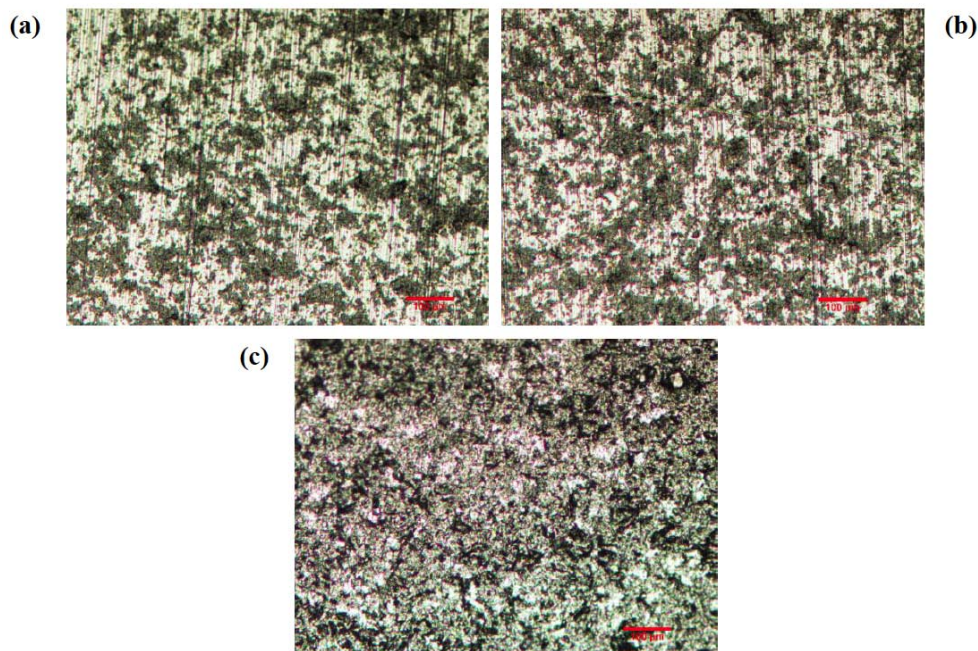
Table S1: The Intensity Correlation Ratios of D to G Peak as well 2D to G, Respectively for the Commercial Examine Samples

Sample	I(D/G)	I(2D/G)
S _A	0.05±0.05	0.43±0.19
S _B	0.04±0.04	0.41±0.13
S _C	0.04±0.05	0.43±0.17

**Figure S3:** XPS survey scans of (i) S_A, (ii) S_B and (iii) S_C samples coated with GRMs as well of graphite.**S3: OM, SEM AFM AND XRD ANALYSIS ON COMMERCIAL AL FOILS COATED WITH GRMs**

By comparing the images of Figure S3, the differences in the homogeneity of the coatings are obvious. It is assumed that the coverage of the samples, S_B and S_C is incomplete.

By comparing the images of Figure S2, the differences in the homogeneity of the coatings are obvious. It is assumed that the coverage of the samples, S_B and S_C is incomplete.

**Figure S4:** OM images for (a) S_A, (b) S_B and (c) S_C. The scale bars are at 100 μm.

Scanning the surface of the samples with the SEM, it provided a better understanding of the coating of each sample. In addition to the information about the non-uniform coating of the aluminum surface by the graphic materials, other morphological observations were observed. Thus, the high roughness of the surfaces due to the inhomogeneous coating of the stationery materials in each sample was found, while in addition, and perhaps most importantly, the incomplete contact of the graphic materials with the aluminum surface.

More specifically, from the SEM image of the S_A sample it appears that the graphitic structures are significantly smaller in size than those of the other two samples. At the same time, in the images of samples S_A and S_B , the rolling lines of aluminum substrate are observed, while in sample S_C this does not occur. These observations indicate that the commercially available samples have undergone different processing both during the rolling of the foil and the application of the graphite materials.

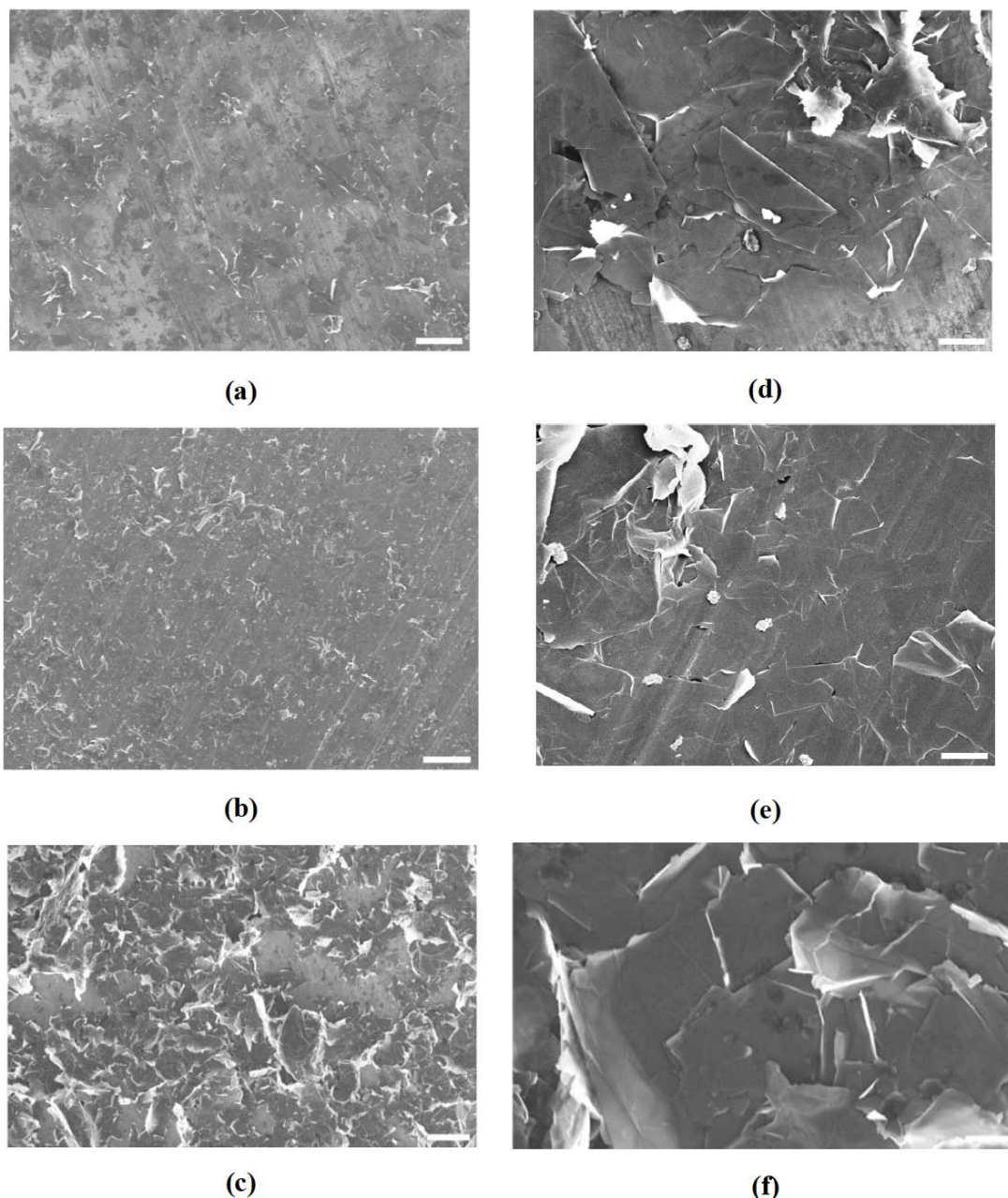


Figure S5: SEM images for S_A with a scale bar at (a) 2 μm and (d) 10 μm , for S_B with a scale bar at (b) 2 μm and (d) 10 μm and S_C with a scale bar at (c) 2 μm and (f) 10 μm , respectively.

From the images with larger magnification areas of the samples (Figure S4d, e, f) the above observations seem to be verified. Also, some of the morphological characteristics of graphitic materials are more visible in these images. More specifically, there are various folds of the graphitic structures, as well as the random way of their deposition on the surface of the metal substrate. At the same time, in all samples it is observed that the graphitic structures are not in full contact with the substrate.

Furthermore, it is clear from the images of the S_C sample that it has a higher roughness than the other two samples, which may be related to the use of a larger amount of material during its coating stage. However, this morphological difference also seems to be related to the thickness of the graphitic structures of the sample, as we saw from the Raman and XPS measurements; this sample seems to have the lowest degree of peeling compared to the other two commercially available samples.

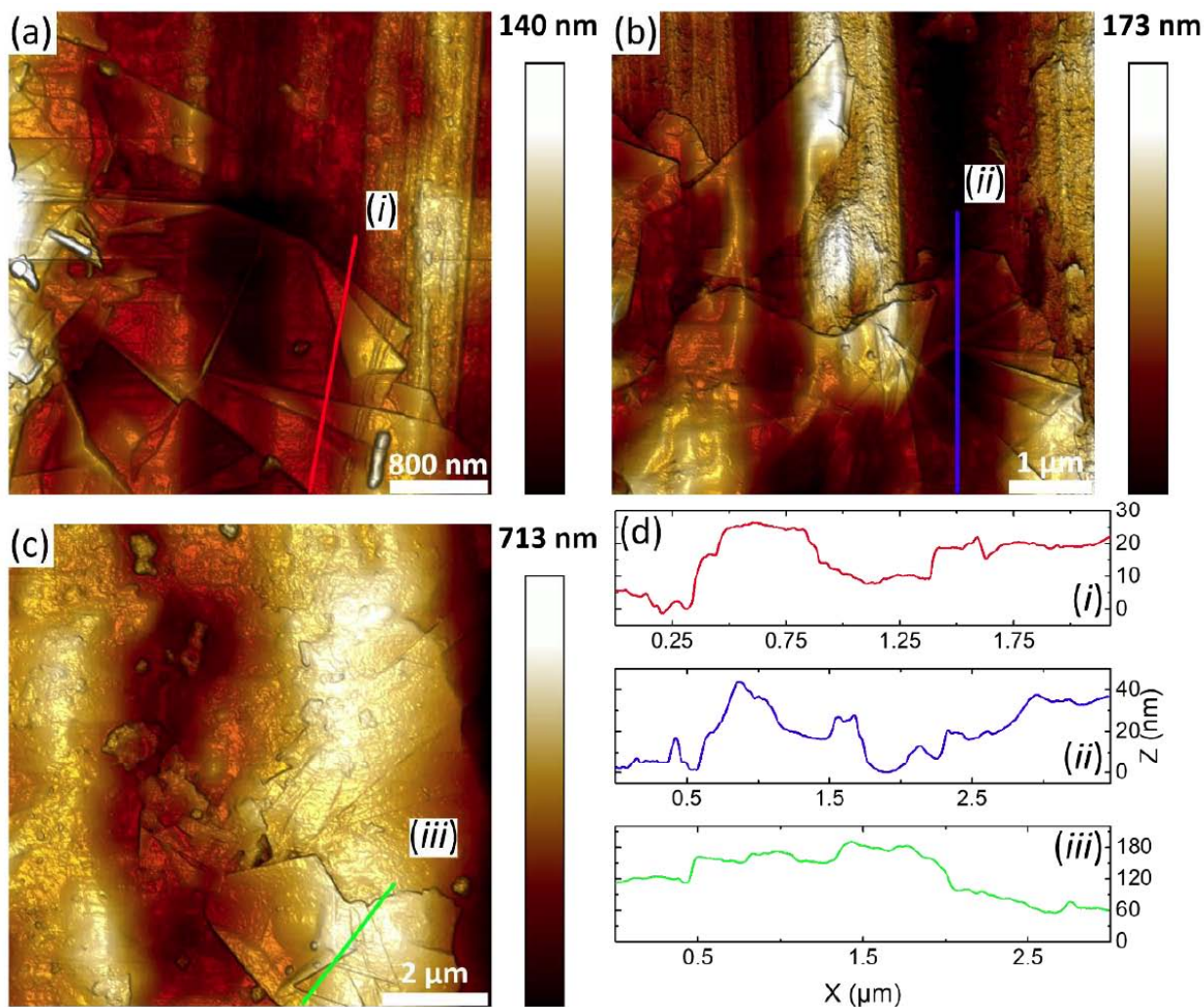


Figure S6: Atomic force microscope (AFM) topography images for commercially available samples. (a) S_A (20 μm), (b) S_B (30 μm), (c) S_C (20 μm). In parentheses, the scale of each image is given. (d) Diagrams of height differences along the lines (i), (ii) and (iii) in (a), (b) and (c), respectively.

In addition to characterization with the above techniques, the samples were also examined using AFM. In Figure S5 typical AFM images from the surface of S_A , S_B και S_C are presented. As seen, in all samples folds and wrinkles graphite nano-structures are observed. Also, as mentioned above, the different morphology of the metal substrate is shown, since in samples S_A and S_B rolled lines are observed, while for S_C are not present.

At the same time, as noted above with the SEM images, these folds do not appear to be in contact with the aluminum surface; thus, creates gaps and voids between the graphite structures and the metal substrate respectively, which could act as local initiation concentrations areas of corrosion.

The morphological differences on the surface of the samples are shown in Figure S4, where the diagrams of the height differences from the sections (i), (ii) and (iii) of the AFM images of each sample are presented, respectively. It is clear that the folds of the graphitic nanostructures in combination with the non-uniformity of the metal substrates create a great roughness in the samples. Regarding the folds of graphitic nanostructures, in all samples it seems to be > 10 nm. However, for the S_C sample in many cases they even reach 30 nm, resulting in the greater number of graphene layers in the nanostructures.

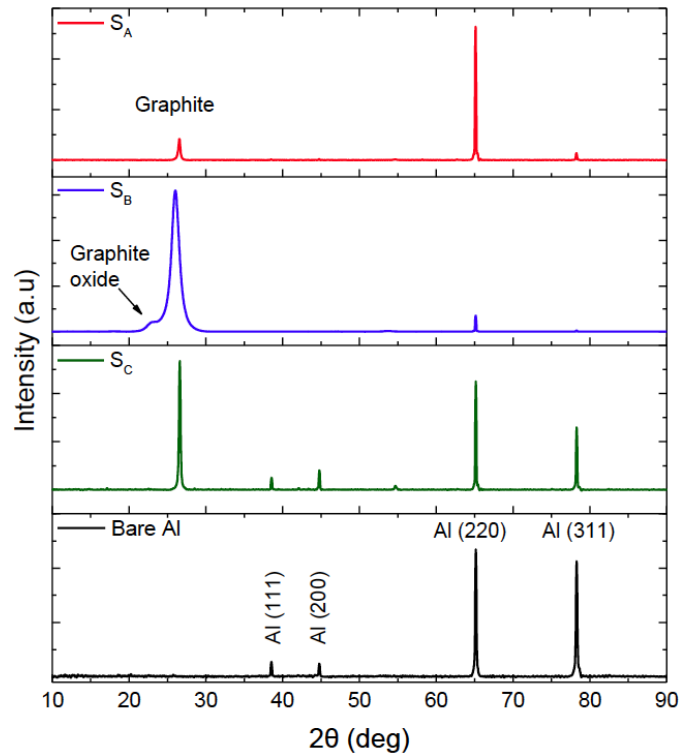


Figure S7: XRD spectra of all commercially Al foils coated with GRMs as well bare Aluminum Al₁₀₀₀.

Finally, X-ray diffraction (XRD) measurements were performed to investigate the crystal structure of the foil substrates, both commercially available samples. As can be seen from the spectra of Figure 1.23, the peak intensities of the crystalline levels of aluminum differ between the samples. However, all samples show peaks at 38°, 44°, 65° and 78° which correspond to the crystallographic levels (111), (200), (220) and (311) of aluminum, respectively [1].

Also, the peak displayed by all commercially available samples at 26° is a typical graphite peak. As can be seen for sample S_B, the peak is wider and shows a shoulder at 22°, confirming conclusions in relation to the greater degree of oxidation of the graphitic material of its coating [2, 3]. These results are expected to affect the corrosion behavior of aluminum substrates.

S4: ANALYSIS OF COATINGS WITH GO AND ITS DERIVATIVES

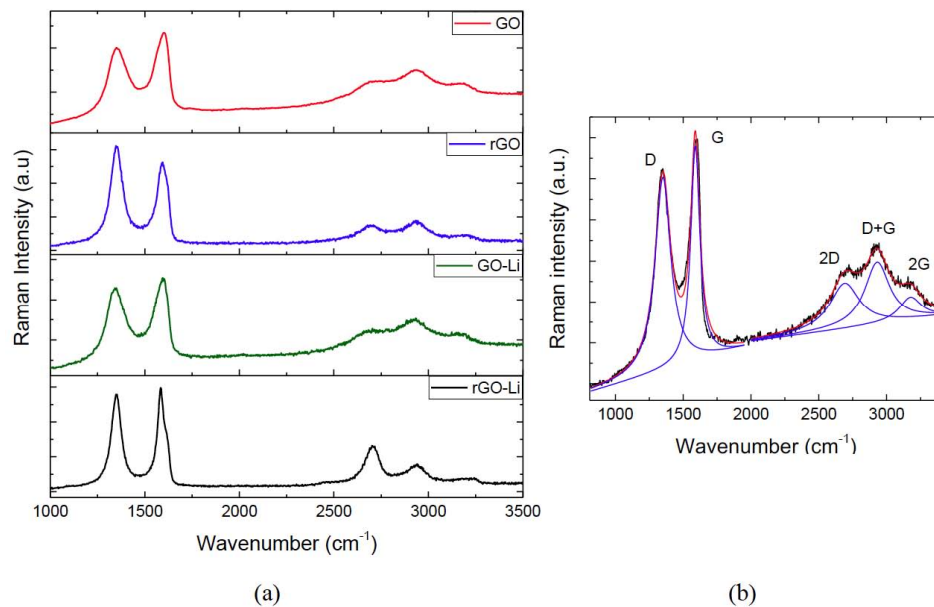


Figure S8: (a) Typical Raman spectra for all samples examined (GO, rGO, GO-Li and rGO-Li) and (b) an example of Raman fitting of GO with the characteristic peaks of D, G, 2D, D+G and 2G.

Figure S7 (b) shows the characteristic Raman peaks of GO. The G peak is located at $\sim 1580\text{ cm}^{-1}$ and is related with the order E_{2g} mode and with the in plane stretching of C=C bonds [4]. The D peak at $\sim 1350\text{ cm}^{-1}$ is related to the breathing mode and its intensity is associated with the number of defects of the lattice [5]. The overtone of D peak is the 2D peak at $\sim 2700\text{ cm}^{-1}$, which is required two-photons scattering for activation. Finally the overtone peaks G+D and 2G are overtones of the combination of D and G peaks and G peak respectively [6].

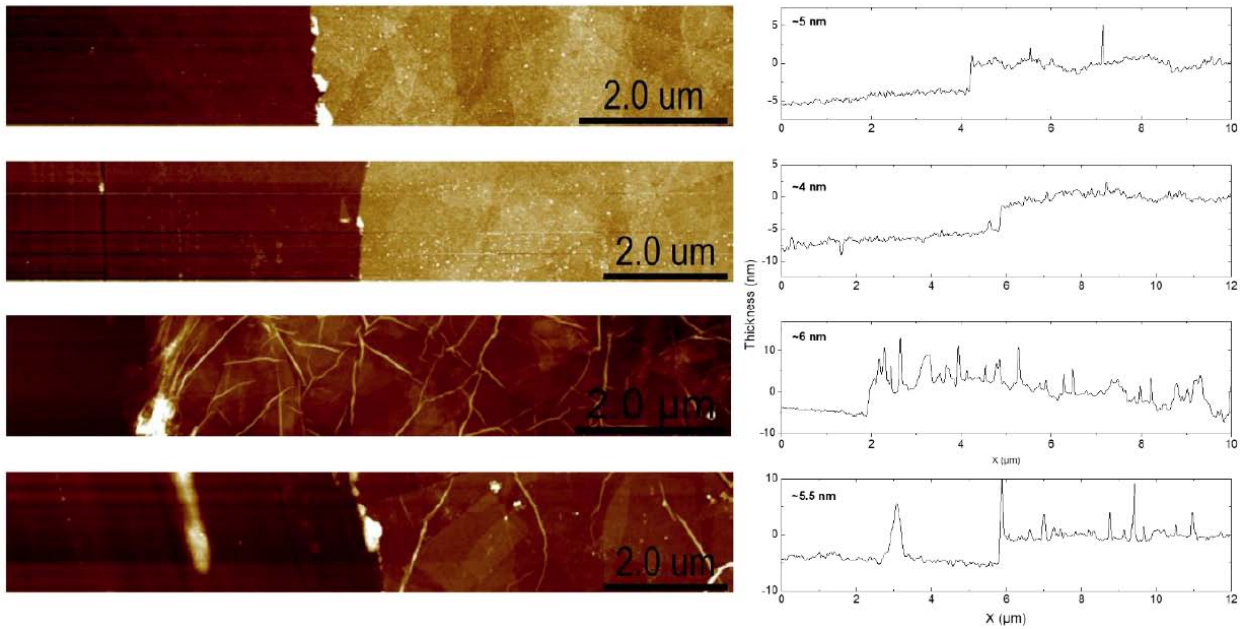


Figure S9: (left) AFM scanning maps and (right) the corresponding thickness distribution for GO, rGO, GO-Li and rGO-Li samples (The scale bar is at 2 μm).

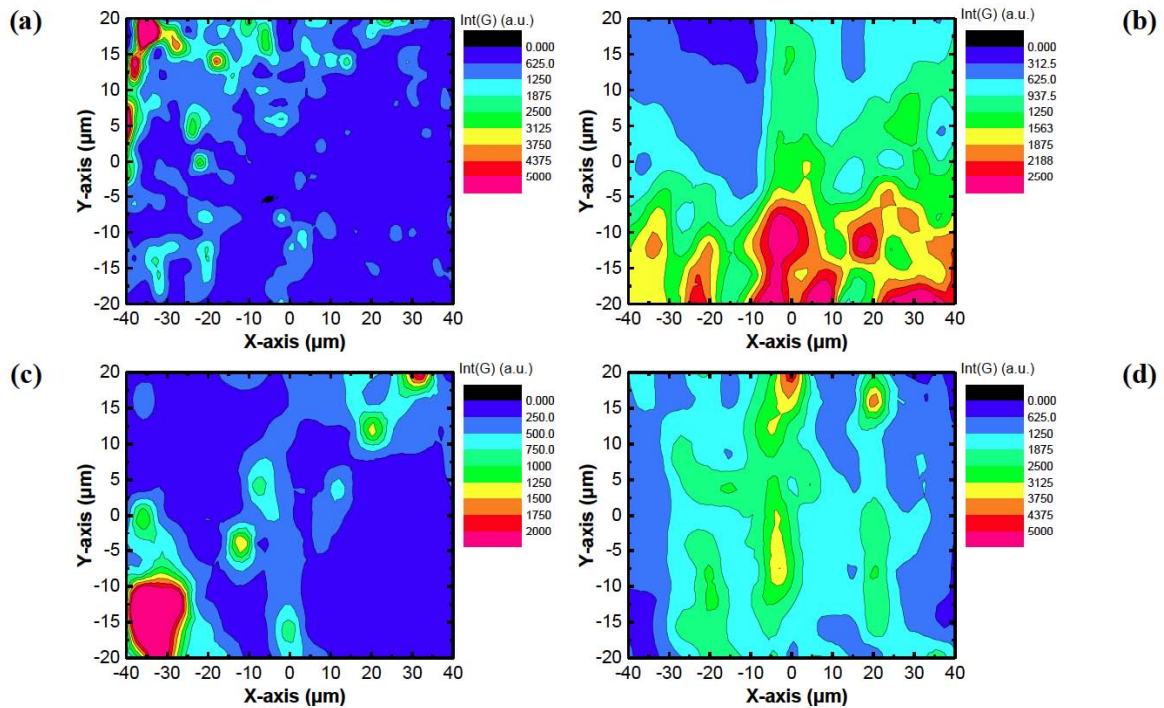


Figure S10: G-peak intensity Raman maps for (a) GO, (b) rGO, (c) GO-Li and (d) rGO-Li, respectively.

REFERENCES

- [1] Narayanasamy R, Ramesh T, Prabhakar M. Effect of particle size of SiC in aluminium matrix on workability and strain hardening behaviour of P/M composite. *Materials Science and Engineering: A* 2009; 504(1): 13-23. <https://doi.org/10.1016/j.msea.2008.11.037>

- [2] Shokrieh MM, Esmkhani M, Shahverdi HR, Vahedi F. Effect of Graphene Nanosheets (GNS) and Graphite Nanoplatelets (GNP) on the Mechanical Properties of Epoxy Nanocomposites. *Science of Advanced Materials* 2013; 5(3): 260-266.
<https://doi.org/10.1166/sam.2013.1453>
- [3] Cui P, Lee J, Hwang E, Lee H. One-pot reduction of graphene oxide at subzero temperatures. *Chemical Communications* 2011; 47(45): 12370-12372.
<https://doi.org/10.1039/C1CC15569E>
- [4] Martins Ferreira EH, Moutinho MVO, Stavale F, Lucchese MM, Capaz RB, Achete CA, Jorio A. Evolution of the Raman spectra from single-, few-, and many-layer graphene with increasing disorder. *Phys Rev B* 2010; 82(12): 125429.
<https://doi.org/10.1103/PhysRevB.82.125429>
- [5] Caçado LG, Jorio A, Ferreira EHM, Stavale F, Achete CA, Capaz RB, Moutinho MVO, Lombardo A, Kulmala TS, Ferrari AC. Quantifying Defects in Graphene via Raman Spectroscopy at Different Excitation Energies. *Nano Lett* 2011; 11(8): 3190-3196.
<https://doi.org/10.1021/nl201432g>
- [6] Ma B, Rodriguez RD, Ruban A, Pavlov S, Sheremet E. The correlation between electrical conductivity and second-order Raman modes of laser-reduced graphene oxide. *Physical Chemistry Chemical Physics* 2019; 21(19): 10125-10134.
<https://doi.org/10.1039/C9CP00093C>